Journal of Applied Physics

Pulsed laser deposition of single layer, hexagonal boron nitride (white graphene, h-BN) on fiber-oriented Ag(111)/$SrTiO_3$(001)

Cite as: J. Appl. Phys. **119**, 095306 (2016); https://doi.org/10.1063/1.4943174
Submitted: 10 November 2015 • Accepted: 21 February 2016 • Published Online: 04 March 2016

Daniel Velázquez, Rachel Seibert, Hamdi Man, et al.

Pulsed laser deposition of single layer, hexagonal boron nitride (white graphene, h-BN) on fiber-oriented Ag(111)/$SrTiO_3$(001)

Daniel Velázquez,[1] Rachel Seibert,[1] Hamdi Man,[1,2] Linda Spentzouris,[1] and Jeff Terry[1]
[1]*Physics Department, Illinois Institute of Technology, Chicago, Illinois 60616, USA*
[2]*Department of Basic Sciences, Turkish Military Academy, Ankara 06654, Turkey*

(Received 10 November 2015; accepted 21 February 2016; published online 4 March 2016)

We report on the growth of 1–10 ML films of hexagonal boron nitride (h-BN), also known as white graphene, on fiber-oriented Ag buffer films on $SrTiO_3$(001) by pulsed laser deposition. The Ag buffer films of 40 nm thickness were used as substitutes for expensive single crystal metallic substrates. *In-situ*, reflection high-energy electron diffraction was used to monitor the surface structure of the Ag films and to observe the formation of the characteristic h-BN diffraction pattern. Further evidence of the growth of h-BN was provided by attenuated total reflectance spectroscopy, which showed the characteristic h-BN peaks at $\sim$780 cm^{-1} and 1367.4 cm^{-1}. *Ex-situ* photoelectron spectroscopy showed that the surface of the h-BN films is stoichiometric. The physical structure of the films was confirmed by scanning electron microscopy. The h-BN films grew as large, sub-millimeter sheets with nano- and micro-sheets scattered on the surface. The h-BN sheets can be exfoliated by the micromechanical adhesive tape method. Spectral analysis was performed by energy dispersive spectroscopy in order to identify the h-BN sheets after exfoliation. The use of thin film Ag allows for reduced use of Ag and makes it possible to adjust the surface morphology of the thin film prior to h-BN growth. © *2016 AIP Publishing LLC*.
[http://dx.doi.org/10.1063/1.4943174]

I. INTRODUCTION

Boron nitride (BN) is a wide band gap ($\sim$5 eV) refractory ceramic often used in high temperature applications such as lubricants due to its chemical stability.[1] Single layer, hexagonal BN (h-BN), also known as white graphene, is a polymorph of interest with a breadth of applications such as photonic, thermo-electronic, and heterostructure devices.[2–4] It has a hexagonal crystalline structure with lattice constant of $\sim$2.5 Å. With roughly a 1.5% mismatch with respect to the lattice of grapheme,[5] the similarity of h-BN to graphene has played a key role in the growth and characterization of both materials on their own as well as the intercalation of h-BN and graphene layers to create novel nano-structures.[6–8] A variety of complex physical and chemical techniques have been used to grow h-BN on diverse ceramic and semiconductor substrates,[9–16] which often bind in a highly interactive manner with the BN film. Nonetheless, the study of h-BN as an isolated system is of importance for potential applications, similar to those of graphene, where conductivity is an issue (i.e., gating devices). Hence, it is important to understand the fundamental properties of the electronic and geometric structure of h-BN in a weakly interactive environment. We used an approach to the synthesis of h-BN that was similar to the deposition of graphene on single crystal Ag. There, the weak interaction between film and substrate allows for the study of graphene as an isolated system.[17]

It has been shown that crystalline Ag surfaces provide ideal metallic platforms for the study of h-BN properties, which is, in particular, due to the vanishing BN-Ag interface energetics, observed both, theoretically and experimentally.[18] In contrast, most other transition metals form highly interactive interfaces with monolayer and bulk BN to the extent that BN often forms superstructured lattices rather than a 2D hexagonal polymorph.[19–28] Although the use of single crystal Ag substrates is viable for the growth of h-BN, it is impractical in the large scale given the high cost of these substrates. In order to circumvent this issue, we have used thin, crystalline, Ag films as growth platforms as substitutes for expensive, single crystal, Ag substrates. We have synthesized h-BN films by Pulsed Laser Deposition (PLD), a state of the art thin film synthesis technique,[29] on 40 nm thick, fiber-oriented Ag(111) buffer layers on $SrTiO_3$(001). The h-BN films were characterized *in-situ* via Reflection High-Energy Electron Diffraction (RHEED) and *ex-situ* by Attenuated Total Reflectance (ATR), Photoelectron Spectroscopy (PES), Energy Dispersive Spectroscopy (EDS), and Scanning Electron Microscopy (SEM).

II. EXPERIMENTAL DETAILS

The experimental growth chamber, shown in Figure 1, is attached to a pumping assembly that includes a turbomolecular pump and an ion pump. The chamber pressure was lower than 2×10^{-9} Torr during deposition. The substrate surface temperature was measured using an optical pyrometer through an IR transmissive viewing port. A Staib Instruments RH15 RHEED system consisting of a remotely controlled electron gun and a phosphor screen was arranged on an axis parallel to the surface of the sample. RHEED patterns were collected with an electron beam energy of 15.2 keV and a current of $\sim$0.2 μA. The electron beam diameter was $\sim$300 μm and was incident at an angle of $\sim$2°.

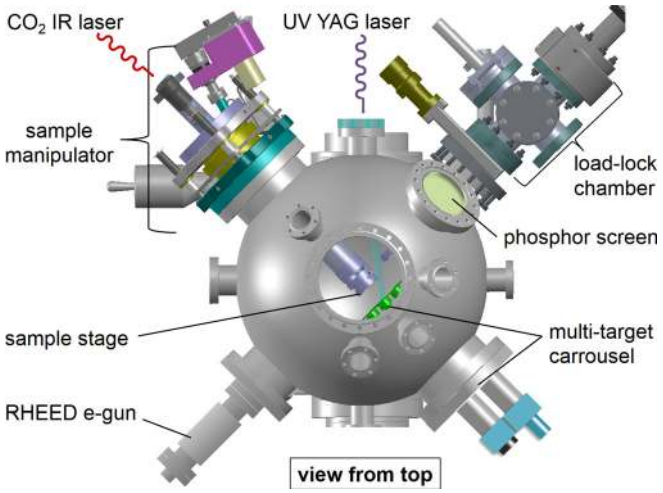

FIG. 1. Schematic drawing of the PLD system.

A remotely controlled multi-target carrousel from Excel Instruments was used to hold six ablation targets for the growth of complex multilayers and superlattices. Ablation was performed using a Continuum Surelite III-10 YAG laser (1064 nm, 850 mJ/pulse) with the second and fourth harmonic generators used to produce 266 nm, 100 mJ/pulse, 5 ns width pulses. The laser is operable at up to 10 Hz with a circular spot size of ∼9 mm in diameter. The laser pulses are directed at UV mirrors and are focused on the target surface inside the chamber with a UV lens (fused silica) at an angle of incidence of 45°. The fluence (pulse energy/ablation spot) was held between 5 and 6 J/cm^2 during deposition. A quartz crystal microbalance (QCM) by Inficon (SQM 160) was used to measure the deposition rate. Prior to deposition on the substrate, the QCM sensor was placed at the substrate position and the deposition rate was calibrated for every film. The deposition rate, independently verified by ellipsometry, was found to be consistent over several weeks with variation of less than 10%.

SEM/EDS were performed using a Phenom Pro X Desktop SEM at 5 kV for surface imaging and spectral analysis at a resolution of 17 nm. Photoelectron spectroscopy measurements were collected using a double-pass cylindrical mirror analyzer (PHI 25–260AR) with a pass energy of 15 eV (with resolution $\Delta E_{det} \cong 0.02PE = 0.3$ eV). The excitation source was a non-monochromatic Al K_α (1486.6 eV with 0.85 eV FWHM) X-ray source (PHI 04–500). The total resolution of the system was 0.9 eV. Attenuated Total Reflectance (ATR) was performed using a Thermo Nicolet Nexus 470 FT-IR. An Omnic Sampler Horizontal Attenuated Total Reflectance (HATR) accessory was attached for ATR mode. The HATR uses a Ge crystal for scans in the range of 4000–600 cm^{-1} at a resolution of 4 cm^{-1}. Data sets consisted of 32 averaged scans per sample.

III. RESULTS AND DISCUSSION

Commercially available, single crystal $SrTiO_3$(001) substrates were used as the platform for the growth of the 40 nm buffer Ag(111) layers and the h-BN film. The $SrTiO_3$(001) substrates were cleaned *in-situ* by IR laser heating to approximately 400 °C. Figure 2(a) shows the RHEED pattern of the clean $SrTiO_3$(001) surface, which displays thin reciprocal lattice rods and Kikuchi lines along the [100] azimuth. The buffer Ag(111) layers were grown at 150 °C with a deposition rate of ∼2 nm per minute (∼9.4 ML/min). The RHEED pattern of Ag(111)/$SrTiO_3$(001) is shown in Figure 2(b), which displays thin modulated and curved rods. This pattern shows superimposed families of rods due to the [211] and [101] azimuths,[30,31] which elucidate the hexagonal lattice of the Ag(111) film and indicate that the film consists of a random azimuthal distribution of Ag(111) normal crystals (i.e., fiber-oriented or 2D polycrystal[31–33]). The curvature of the rods, away from the sample surface shadow (bottom of RHEED pattern) are, in fact, the result of the intersection of the Ewald sphere with reciprocal lattice cylinders, which provide further evidence of the azimuthal randomness of normally oriented, Ag(111) crystalline faces. Boron nitride films were deposited at 200 °C, with a deposition rate of 0.7 nm per minute (∼2 ML/min), on the fiber-oriented

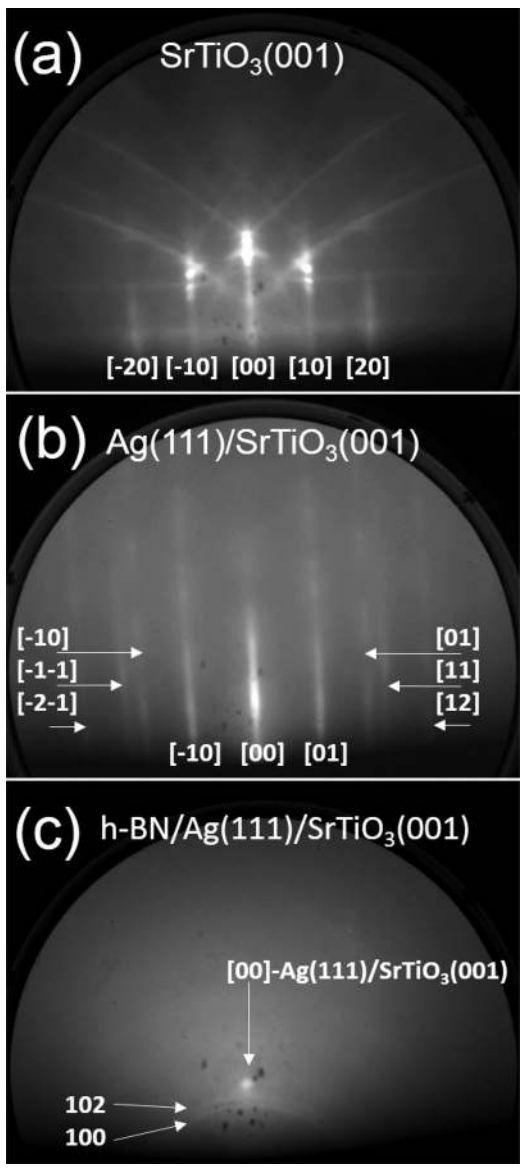

FIG. 2. RHEED patterns of (a) clean $SrTiO_3$(001) substrate, (b) fiber-oriented Ag(111)/$SrTiO_3$(001), and (c) h-BN/Ag(111)/$SrTiO_3$(001).

Ag(111)/$SrTiO_3$(001). Figure 2(c) shows the RHEED pattern of a 10 monolayer (ML) thick (33.3 Å) BN film, which exhibits the [100] and [102] rings of h-BN.[9,18,34] Also visible is the specular spot of Ag(111)/$SrTiO_3$(001). In general, the sharpness of all RHEED pattern features presented are indicative of highly ordered surfaces.

Figure 3(a) shows a 5 keV SEM image of h-BN/Ag(111)/$SrTiO_3$(001). For this sample, BN and Ag were deposited at slightly different angles to produce a shadow effect using a metallic tab in order to leave the Ag layer partially uncoated. The fiber texture of the Ag layer, anticipated from RHEED (Figure 2(b)), is manifested in the physical structure of the film which consists of a random azimuthal distribution of crystallites. The appearance of rings rather than rods in the RHEED pattern of the h-BN film seen in Figure 2(c) is due to the formation of h-BN nano-sheets and nano-flakes on an underlying uniform h-BN layer. The underlying layer thus likely forms through the 2D growth of smaller h-BN domains which coalesced to cover large areas. The interaction of the h-BN domains and the Ag surface is weak due to the interplay of electrostatic repulsion and van der Waals forces balancing beyond typical covalent bonding distances and thus, inhibiting the influence of the substrate on the azimuthal orientation of h-BN.[35]

In order to examine the h-BN films independently from the Ag(111)/$SrTiO_3$(001) growth platforms, they were exfoliated using the adhesive tape method often employed to cleave graphene.[36,37] To facilitate exfoliation, the films were heated up to 400 °C for 1 min. Figure 3(b) shows a 5 keV SEM image of the exfoliated h-BN film which consists of large sub-millimeter fragmented sheets, likely due to fracture of crystallite boundaries during lift off. Figure 3(c) shows 5 keV EDS spectra acquired at sample points on one of the BN fragments and uncovered adhesive tape. The drastic change of concentrations observed from the C K_α and N K_α peaks indicate that the flat regions with lighter shade (Figure 3(b)) are BN despite the insensitivity of EDS to boron. The ability to readily exfoliate large h-BN domains from epitaxially grown films improves the likelihood of this technique being used in industrial applications.

In addition to spectral analysis by EDS, PES was used to characterize the chemical structure of the films *ex-situ*.[38,39] Samples were exposed to air momentarily during transfer from the PLD deposition chamber to the PES analysis chamber. The atomic ratio of B:N for the h-BN films was calculated to be 1.1. This calculation was performed using PES data obtained from a commercially available (Sigma Aldrich) h-BN reference sample. Figure 4 shows narrow scans of the (a) O 1 s, (b) N 1 s, (c) C 1 s, and (d) B 1 s core levels and their respective fits collected using a photon energy of 1486.6 eV. The components of elemental peaks from the film, that is, N 1 s and B 1 s, indicate that the main film impurity was adventitious oxygen, as evidenced by the electron density shifts toward lower kinetic energy due to oxidation.[10,12,40–43] Additional surface contaminants are adventitious carbon and water, which did not directly interact with the film as shown by the electron density shifts in the O 1 s and C 1 s core levels due to CO, CO_2, and hydroxides.[42–44] Oxidation and surface impurities were attributed to

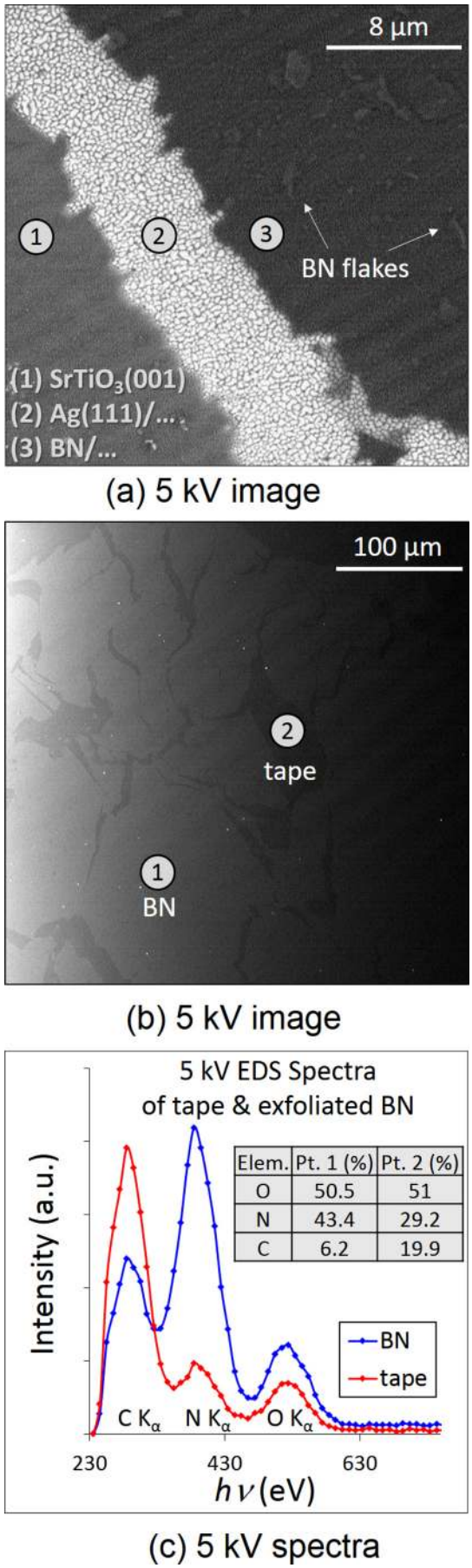

FIG. 3. SEM images of (a) h-BN/Ag(111)/$SrTiO_3$(001), (b) exfoliated h-BN, and (c) EDS spectra of exfoliated h-BN and adhesive tape.

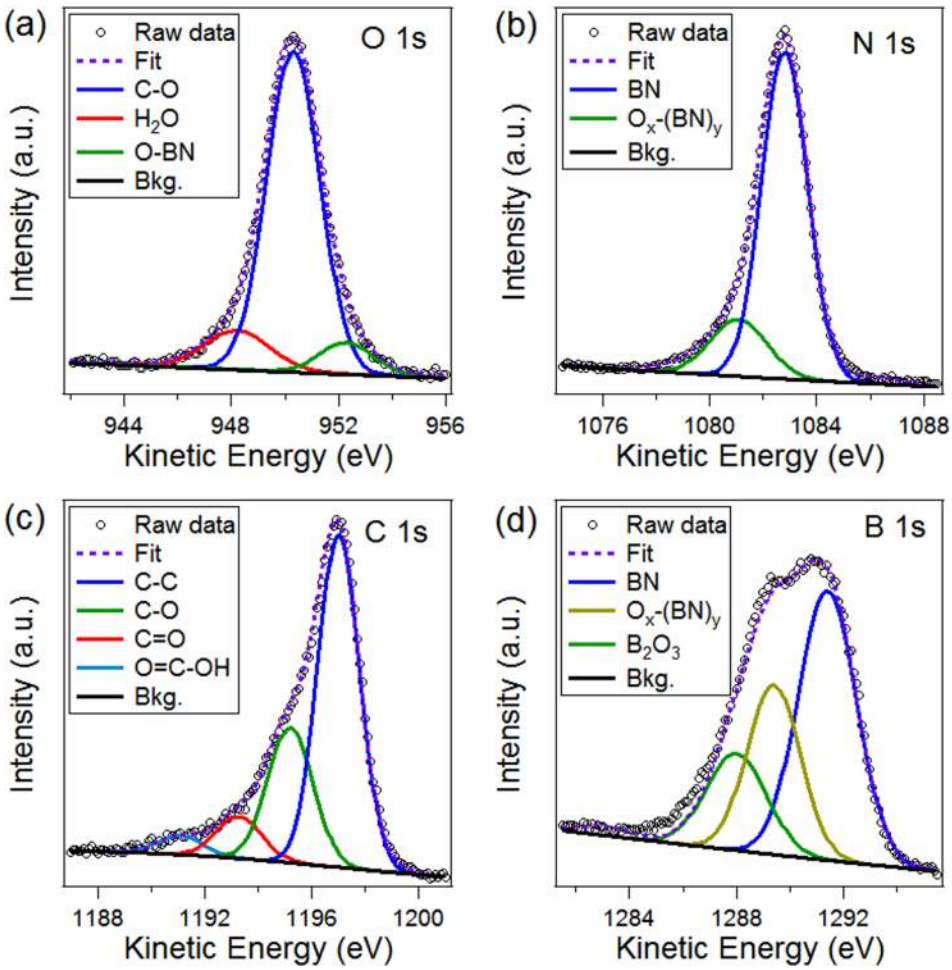

FIG. 4. PES of h-BN/Ag(111)/$SrTiO_3$(001) using a photon energy of 1486.6 eV shows narrow scan fits and decomposition of the (a) O 1 s, (b) N 1 s, (c) C 1 s, and (d) B 1 s core level envelopes.

the brief exposure to air during transport for analysis. In addition, peak broadening to some extent was likely due to flaking and nano-sheet formation. Thus, it is evident that the surface contaminants did not affect the chemistry of the h-BN films, which remained stoichiometric. Table I summarizes the assignments of the peak components for each core level, their kinetic energies (and corresponding binding energies) as well as references used in the criteria for peak assignment.

In order to show the growth of ultra-thin films, and as additional and direct evidence of the formation of the hexagonal polymorph of BN, we used attenuated total reflectance infrared spectroscopy to study films of thicknesses of 1, 2, and 10 ML. Previously, Gorbachev *et al.*[45] have shown that it is possible to identify single and multilayer h-BN by tracking small shifts in the position of the characteristic E_{2g} (in-plane) phonon mode peak at for h-BN, usually observed around 1367 cm^{-1}.[11,41,42,46,47] Figure 5(a) shows ATR spectra of 0, 1, 2, and 10 ML of h-BN deposited on Ag(111)/$SrTiO_3$(001). The characteristic features of h-BN[10,42,47] are immediately evident on the bulk spectrum (10 ML); the out-of-plane and in-plane modes at 780 cm^{-1} and 1367.4 cm^{-1}, respectively. Figure 5(b) shows a narrowed version of Figure 5(a) in order to focus on the position of the in-plane peak. For emphasis, only the spectrum of bulk h-BN (10 ML) was scaled (1/100), and all spectra have been stacked (i.e., Relative Transmittance). Fits for the spectra of 1 and 2 ML films are superimposed as viewing guides. As expected, the in-plane peak is absent in the spectrum of Ag(111) $SrTiO_3$(001) (i.e., 0 ML). Furthermore, the position of the in-plane peak is modulated in accordance with the h-BN film thickness; at 1 ML the peak appears at slightly higher wavenumber (1371.7 cm^{-1}) with respect to the bulk value and at 2 ML it shifts to a slightly lower value (1357.7 cm^{-1}) with some extent of broadening likely due to scarce domains of 1 and perhaps 3 ML. These observations are consistent with those previously reported[45] and confirm the ability to grow single layer h-BN.

TABLE I. Component assignments of PES core level peaks of h-BN film on Ag(111)/$SrTiO_3$(001) (Photon energy: 1486.6 eV).

Core level	Component assignment	KE (eV)	BE (eV)	Reference
O 1 s	O-BN	952.2	529.4	10 and 40
	C-O	950.3	531.3	
	H_2O	948.0	533.6	
N 1 s	BN	1082.8	398.8	10, 12, 40, 41, and 43
	O_x-$(BN)_y$	1081.4	400.2	
C 1 s	C-C	1197.0	284.6	42 and 44
	C-O	1195.2	286.4	
	C = O	1193.3	288.3	
	O = C-OH	1191.1	290.5	
B 1 s	BN	1291.4	190.2	12, 40, 41, and 43
	O_x-$(BN)_y$	1289.4	192.2	
	B_2O_3	1288.0	193.6	

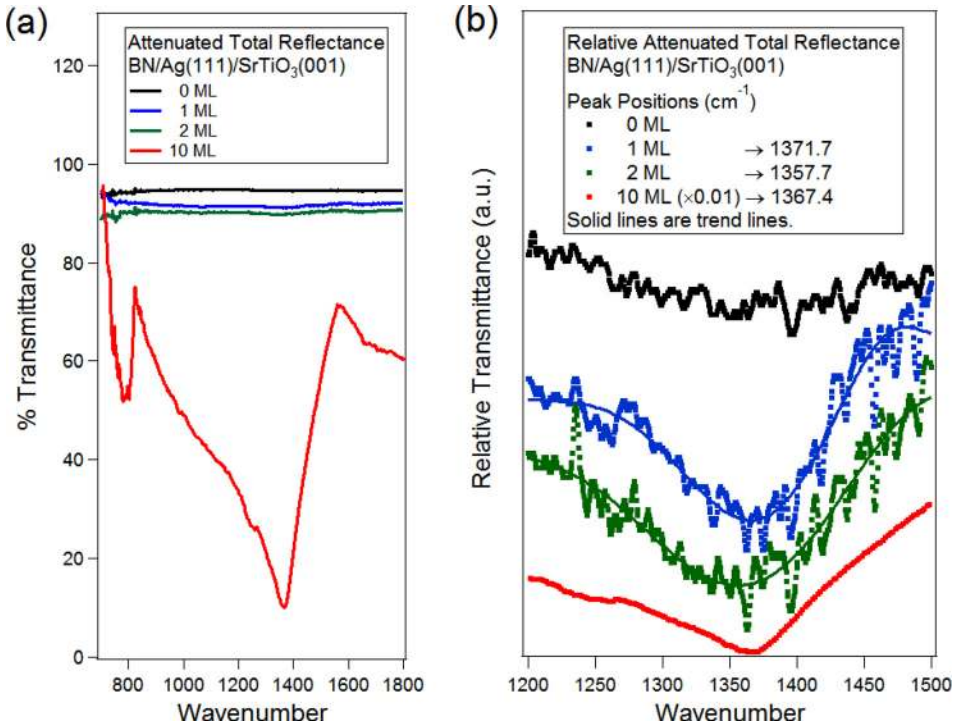

FIG. 5. Transmittance mode ATR of 1, 2, and 10 ML h-BN films on Ag(111)/$SrTiO_3$(001): (a) superimposed raw spectra; (b) scaled transmittance of 1, 2 and 10 ML sample films.

Our characterization of 1–10 ML films of hexagonal boron nitride has shown that pulsed laser deposition can be used to controllably deposit 1–10 ML films of h-BN on fiber-oriented Ag(111)/$SrTiO_3$(001). The 1 ML boron nitride films, known as white grapheme, can be easily exfoliated. The use of the thin silver films greatly reduces the amount of silver needed in the synthesis of the h-BN. This synthesis of h-BN may be of interest to those needing a non-conductive single layer compound to be paired with graphene in single atomic layer nano-devices.

IV. CONCLUSION

We have presented evidence for the growth of h-BN films using pulsed laser deposition on fiber-oriented Ag(111)/$SrTiO_3$(001) through the use of physical (RHEED, SEM, and ATR) and chemical (PES and EDS) characterization techniques. The ability to grow h-BN on a 2D-polycrystalline Ag(111) surface highlights the weak interaction of the film with Ag and provides an ideal platform for the study of h-BN in isolation. This also emphasizes the potential of using inexpensive Ag films to grow h-BN as substitutes for single crystal Ag substrates. In addition, post-deposition annealing facilitated micromechanical exfoliation of large multilayer h-BN domains, which allowed for the close examination of h-BN and opens the possibility of simplifying the process of growth and exfoliation for potential future applications in nano-devices. We also proved the formation of monolayer h-BN by tracking the thickness-dependent modulatory behavior of the in-plane phonon mode peak through the use of ATR. This result reiterates the efficacy of the Ag(111) films as growth surfaces even for the synthesis of atomically thin layers.

ACKNOWLEDGMENTS

The authors thank Aditya Unni, Adam Hock, José Orozco, and Frank Harwarth for valuable discussions and the facilitation of resources crucial for the completion of these studies. This work was funded by the National Science Foundation under Grant No. 0969989, the Department of Energy under Grant No. DE-SC0007952, and the U.S. Department of Education through the GAANN Fellowship Program Award No. P200A090137.

[1]S. Alkoy, C. Toy, T. Gonul, and A. Tekin, "Crystallization behavior and characterization of turbostratic boron nitride," J. Eur. Ceram. Soc. **17**(12), 1415–1422 (1997).
[2]H. X. Jiang and J. Y. Lin, "Hexagonal boron nitride for deep ultraviolet photonic devices," Semicond. Sci. Technol. **29**, 084003 (2014).
[3]C.-C. Chen, Z. Li, L. Shi, and S. B. Cronin, "Thermoelectric transport across graphene/hexagonal boron nitride/graphene heterostructures," Nano Res. **8**(2), 666–672 (2015).
[4]M. S. Choi, G. H. Lee, Y. J. Yu, D. Y. Lee, S. H. Lee, P. Kim, J. Hone, and W. J. Yoo, "Controlled charge trapping by molybdenum disulphide and graphene in ultrathin heterostructured memory devices," Nat. Commun. **4**, 1624 (2013).
[5]Y. Kobayashi, T. Akasaka, and T. Makimoto, "Hexagonal boron nitride grown by MOVPE," J. Cryst. Growth **310**, 5048–5052 (2008).
[6]L. Ci, L. Song, C. Jin, D. Jariwala, D. Wu, Y. Li, A. Srivastava, Z. F. Wang, K. Storr, L. Balicas, F. Liu, and P. M. Ajayan, "Atomic layers of hybridized boron nitride and graphene domains," Nat. Mater. **9**, 430–435 (2010).
[7]J. Park, J. Lee, L. Liu, K. W. Clark, C. Durand, C. Park, B. G. Sumpter, A. P. Baddorf, A. Moshin, M. Yoon, G. Gu, and A. Li, "Spatially resolved one-dimensional boundary states in graphene–hexagonal boron nitride planar heterostructures," Nat. Commun. **5**, 5403 (2014).
[8]A. G. F. Garcia, M. Neumann, F. Amet, J. R. Williams, K. Watanabe, T. Taniguchi, and D. Goldhaber-Gordon, "Effective cleaning of hexagonal boron nitride for graphene devices," Nano Lett. **12**(9), 4449–4454 (2012).
[9]T. Oku, "Synthesis, atomic structures and properties of boron nitride nanotubes," in *Physical and Chemical Properties of Carbon Nanotubes* (InTech, 2013), pp. 119–153.

[10]A. Anzaia, F. Nishiyamab, S. Yamanaka, and K. Inumarua, "Thin film growth of boron nitride on α-Al_2O_3(001) substrates by reactive sputtering," Mater. Res. Bull. **46**(12), 2230–2234 (2011).
[11]L. Song, L. Ci, H. Lu, P. B. Sorokin, C. Jin, J. Ni, A. G. Kvashnin, D. G. Kvashnin, J. Lou, B. I. Yakobson, and P. M. Ajayan, "Large scale growth and characterization of atomic hexagonal boron nitride layers," Nano Lett. **10**(8), 3209–3215 (2010).
[12]N. Guo, J. Wei, L. Fan, Y. Jia, D. Liang, H. Zhu, K. Wang, and D. Wu, "N. Guo, J. Wei, L. Fan, controllable growth of triangular hexagonal boron nitride domains on copper foils by an improved low-pressure chemical vapor deposition method," Nanotechnology **23**, 415605 (2012).
[13]J. D. Ferguson, A. W. Weimer, and S. M. George, "Atomic layer deposition of boron nitride using sequential exposures of BCl_3 and NH_3," Thin Solid Films **413**, 16–25 (2002).
[14]J. Olander, L. M. Ottosson, P. Heszler, J.-O. Carlsson, and K. M. Larsson, "Laser-assisted atomic layer deposition of boron nitride thin films," Chem. Vapor Depos. **11**, 330–337 (2005).
[15]J.-X. Deng, L. Chen, C. Man, L. Kong, M. Cui, and X.-F. Gao, "Deposition of hexagonal boron nitride thin films on silver nanoparticle substrates and surface enhanced infrared absorption," Chin. Phys. B **23**, 047104 (2014).
[16]B. BenMoussa, J. D'Haen, C. Borschel, M. Saitner, A. Soltani, V. Mortet, C. Ronning, M. D'Olieslaeger, H.-G. Boyen, and K. Haenen, "Hexagonal Boron Nitride Nanowalls Synthesized by Unbalanced RF Magnetron Sputtering," in Materials Research Society Fall Meeting, Boston (2010).
[17]B. Kiraly, E. V. Iski, A. J. Mannix, B. L. Fisher, M. C. Hersam, and N. P. Guisingers, "Solid-source growth and atomic-scale characterization of graphene on Ag(111)," Nat. Commun. **4**, 2804 (2013).
[18]F. Müller and S. Grandthyll, "Monolayer formation of hexagonal boron nitride on Ag(001)," Surf. Sci. **617**, 207–210 (2013).
[19]A. B. Preobrajenski, A. S. Vinogradov, M. L. Ng, E. Ćavar, R. Westerström, A. Mikkelsen, E. Lundgren, and N. Mårtensson, "Influence of chemical interaction at the lattice-mismatched h−BN/Rh(111) and h−BN/Pt(111) interfaces on the overlayer morphology," Phys. Rev. B **75**, 245412 (2007).
[20]A. Goriachko, M. K. Yunbin, H. Over, M. Corso, T. Brugger, S. Berner, J. Osterwalder, and T. Greber, "Self-assembly of a hexagonal boron nitride nanomesh on Ru(0001)," Langmuir **23**(6), 2928–2931 (2007).
[21]W. Auwärter, T. Kreutz, T. Greber, and J. Osterwalder, "XPD and STM investigation of hexagonal boron nitride on Ni(111)," Surf. Sci. **429**(1–3), 229–236 (1999).
[22]A. Nagashima, N. Tejima, Y. Gamou, T. Kawai, and C. Oshima, "Electronic structure of monolayer hexagonal boron nitride physisorbed on metal surfaces," Phys. Rev. Lett. **75**, 3918 (1995).
[23]M. Morscher, M. Corso, T. Greber, and J. Osterwalder, "Formation of single layer h-BN on Pd(111)," Surf. Sci. **600**(16), 3280–3284 (2006).
[24]F. Müller, S. Hüfner, and H. Sachdeva, "One-dimensional structure of boron nitride on chromium (110)—A study of the growth of boron nitride by chemical vapour deposition of borazine," Surf. Sci. **602**(22), 3467–3476 (2008).
[25]M. P. Allan, S. Berner, M. Corso, T. Greber, and J. Osterwalder, "Tunable self-assembly of one-dimensional nanostructures with orthogonal directions," Nanoscale Res. Lett. **2**, 94–99 (2007).
[26]T. Greber, L. Brandenberger, M. Corso, A. Tamai, and J. Osterwalder, "Single layer hexagonal boron nitride films on Ni(110)," Surf. Sci. Nanotechnol. **4**, 410–413 (2006).
[27]N. A. Vinogradov, A. A. Zakharov, M. L. Ng, A. Mikkelsen, E. Lundgren, N. Mårtensson, and A. B. Preobrajenski, "One-dimensional corrugation of the h-BN Monolayer on Fe(110)," Langmuir **28**(3), 1775–1781 (2012).
[28]S. Joshi, D. Ecija, R. Koitz, M. Iannuzzi, A. P. Seitsonen, J. Hutter, H. Sachdev, S. Vijayaraghavan, F. Bischoff, K. Seufert, J. V. Barth, and W. Auwärter, "Boron nitride on Cu(111): An electronically corrugated monolayer," Nano Lett. **12**(11), 5821–5828 (2012).
[29]R. Eason, *Pulsed Laser Deposition of Thin Films: Applications-Led Growth of Functional Materials* (John Wiley & Sons, Hoboken, NJ, USA, 2007).
[30]D. Velazquez, R. Seibert, Z. Yusof, J. Terry, and L. Spentzouris, "Synthesis of ultra-thin single crystal MgO/Ag/MgO multilayer for controlled photocathode emissive properties," in International Particle Accelerator Conference, Richmond, VA, USA (2015).
[31]A. Ichimiya and P. I. Cohen, *Reflection High Energy Electron Diffraction* (Cambridge University Press, New York, NY, USA, 2004), pp. 270–313.
[32]R. C. Sundahl and L. Berrin, "Analysis and characterization of ceramic surfaces for electronic applications," in Symposium on the Science of Ceramic Machining and Surface Finishing, Gaithersburg, MD (1970).
[33]G.-C. Wang and T.-M. Lu, "RHEED transmission mode and RHEED Pole Figure," in *RHEED Transmission Mode and Pole Figures: Thin Film and Nanostructure Texture Analysis* (Springer, New York, NY, 2013), p. 73.
[34]O. Dugne, S. Prouhet, A. Guette, R. Naslain, R. Fourmeaux, K. Hssein, J. Sevely, C. Guimon, D. Gonbeau, and G. Pfister-Guillouzo, "AES, XPS and TEM characterization of boron nitride deposited under chemical vapor infiltration (CVI) conditions," J. Phys. Colloq. **50**(C5), C5-333–C5-341 (1989).
[35]F. Müller, S. Hüfner, H. Sachdev, R. Laskowski, P. Blaha, and K. Schwarz, "Epitaxial growth of hexagonal boron nitride on Ag(111)," Phys. Rev. B **82**, 113406 (2010).
[36]K. S. Novoselov, A. K. Geim, S. V. Morozov, D. Jiang, Y. Zhang, S. V. Dubonos, I. V. Grigorieva, and A. A. Firsov, "Electric field effect in atomically thin carbon films," Science **306**, 666–669 (2004).
[37]J. Bohr, "Adhesive tape exfoliation: Why it works for graphene," EPL **109**, 58004 (2015).
[38]S. Hüfner, *Photoelectron Spectroscopy: Principles and Applications* (Springer-Verlag, Berlin, 1995).
[39]J. Terry, R. K. Schulze, J. D. Farr, T. Zocco, K. Heinzelman, E. Rotenberg, D. K. Shuh, G. Van der Laan, D. A. Arena, and J. G. Tobin, "5f resonant photoemission from plutonium," Surf. Sci. **499**, L141 (2002).
[40]D. J. Joyner and D. M. Hercules, "Chemical bonding and electronic structure of B_2O_3, H_3BO_3, and BN: An ESCA, Auger, SIMS and SXS study," J. Chem. Phys. **72**, 1095 (1980).
[41]N. R. Glavin, M. L. Jespersen, M. H. Check, J. Hu, A. M. Hilton, T. S. Fisher, and A. A. Voevodin, "Synthesis of few-layer, large area hexagonal-boron nitride by pulsed laser deposition," Thin Solid Films **572**, 245–250 (2014).
[42]W. Jin, W. Zhang, Y. Gao, G. Liang, A. Gu, and L. Yuan, "Surface functionalization of hexagonal boron nitride and its effect on the structure and performance of composites," Appl. Surf. Sci. **270**, 561–571 (2013).
[43]D. Schild, S. Ulrich, J. Ye, and M. Stüber, "XPS investigations of thick, oxygen-containing cubic boron nitride coatings," Solid State Sci. **12**, 1903–1906 (2010).
[44]H. Ganegoda, D. S. Jensen, D. Olive, L. Cheng, C. U. Segre, M. R. Linford, and J. Terry, "Photoemission studies of fluorine functionalized porous graphitic carbon," J. Appl. Phys. **111**, 053705 (2012).
[45]R. V. Gorbachev, I. Riaz, R. R. Nair, R. Jalil, L. Britnell, B. D. Belle, E. W. Hill, K. S. Novoselov, K. Watanabe, T. Taniguchi, A. K. Geim, and P. Blake, "Hunting for monolayer boron nitride: Optical and Raman signatures," Small **7**(4), 465–468 (2011).
[46]R. Y. Tay, S. H. Tsang, M. Loeblein, W. L. Chow, G. C. Loh, J. W. Toh, S. L. Ang, and E. H. T. Teo, "Direct growth of nanocrystalline hexagonal boron nitride films on dielectric substrates," Appl. Phys. Lett. **106**, 101901 (2015).
[47]M. C. Polo, G. Sanchez, W. L. Wang, J. Esteve, and J. L. Andújar, "Growth of diamond films on boron nitride thin films by bias-assisted hot filament chemical vapor deposition," Appl. Phys. Lett. **70**, 1682 (1997).